

# Mechanics of tissue competition: Interfaces stabilize coexistence

Nirmalendu Ganai<sup>1,2</sup>, Tobias Büscher<sup>1</sup>, Gerhard Gompper<sup>1</sup>, and Jens Elgeti<sup>1,\*</sup>

<sup>1</sup>*Theoretical Soft Matter and Biophysics, Institute of Complex Systems,  
Forschungszentrum Jülich and JARA, 52425 Jülich, Germany and*

<sup>2</sup>*Department of Physics, Nabadwip Vidyasagar College, Nabadwip, Nadia 741302, India*

(Dated: October 1, 2018)

Mechanical forces influence the dynamics of growing tissues. Computer simulations are employed to study the importance of interfacial effects in tissue competition. It was speculated that mechanical pressure determines the competition, where the determining quantity is the homeostatic pressure - the pressure where division and apoptosis balance; the tissue with the higher homeostatic pressure overwhelms the other. Surprisingly, a weaker tissue can persist in stable coexistence with a stronger tissue, if adhesion between them is small enough. An analytic continuum description can quantitatively describe the underlying mechanism and reproduce the resulting pressures and cell-number fractions. Computer simulations furthermore display a variety of coexisting structures, ranging from spherical inclusions to a bicontinuous state.

Mechanical forces influence the growth of cells and tissues in several ways [1–3]. This ranges from plants adapting their growth patterns to mechanical loads [4, 5], all the way to tumor growth responding to mechanical forces [6–8]. Cells have been shown to differentiate according to substrate stiffness [9], and divide according to mechanical stress and strain [10–16]. Spheroids of many cells, grown in elastic gels [17–19] or shells [20, 21], or even in suspension with osmotic stress [22–25], show strong dependence of growth on the mechanical stress from the embedding medium.

Given the evidence of mechanical stress on growth, it seems clear that mechanics should also influence tissue competition, such as the competition between different mutants in the imaginal wing disk of drosophila [26, 27], or clonal expansion in multistep cancerogenesis [28, 29]. Several theoretical studies suggested mechanics as the underlying mechanism for both, competition [1] and size determination [30] in the wing, and tumor growth [8, 31].

Growth is a change of volume and the conjugate force to volume is pressure. It stands to reason that pressure should influence growth. A tissue grown in a finite compartment exerts a certain pressure onto its surrounding. When reaching a steady state - the homeostatic state - this is the homeostatic pressure  $P_H$ . Under an external pressure  $P$  below this value, the tissue grows; whereas it shrinks if the pressure is above it. This simple approach can be formulated as a linear expansion of the bulk growth rate  $k_b$  around the homeostatic pressure [31],

$$k_b = \kappa(P_H - P) \quad (1)$$

with the pressure response factor  $\kappa$ . This idea has been developed to understand mechanical tissue competition in general, and metastatic inefficiency in particular: It was argued that metastases need to reach a critical size, below which the Laplace pressure from the interfacial tension exceeds the homeostatic pressure difference, and the metastasis disappears [31]. To study the role of pressure on growth, experiments and computer simulations have

been developed to explore this effect in cell culture and in silico [22–24, 32–34]. While confirming the general assumption - that mechanical pressure reduces growth - these experiments and simulations have led to another important revelation. Tissues preferentially divide at the surface, even to the extent that they die (on average) in the bulk and sustain a finite size only by surface growth. While consideration of nutrient transport may be necessary for quantitative description of some experiments [35], mechanics alone already suffice.

In this work, we study the role of interfacial effects on mechanical tissue competition by numerical simulations, in particular the effect of adhesive interactions between different tissues. We find that similar to free surfaces, cells divide preferentially at the low-adhesive interface. This interfacial growth in turn can stabilize coexistence of two tissues with different homeostatic pressures.

Agent-based modelling of tissue growth has been very successful in the recent years [36, 37]. We follow the approach of Ref. [32] and model growing and dividing cells by two point-like particles, which repel each other with a growth force  $\mathbf{F}_{ij}^G = \frac{G}{(r_{ij} + r_0)^2} \hat{\mathbf{r}}_{ij}$ . Once a critical distance is reached, cells divide, and two new particles are inserted, starting the process anew. Apoptosis is modeled by a constant rate of cell removal  $k_a$ . Volume exclusion is maintained by a relatively soft repulsive force  $\mathbf{F}_{ij}^V = f_0 \left( \frac{R_{PP}^5}{r_{ij}^5} - 1 \right) \hat{\mathbf{r}}_{ij}$ , while adhesion between cells is modeled by a constant attractive force  $\mathbf{F}_{ij}^A = -f_1 \hat{\mathbf{r}}_{ij}$  between all cells in range  $R_{PP}$ . This model results in pressure-dependent growth, in reasonable agreement with experiments [22–24, 32–34]. For two competing tissues A and B, parameters for each tissue can be set independently. In this work, we only vary the growth strength  $G^A$  and  $G^B$ , the self adhesion strengths,  $f_1^{AA}$ ,  $f_1^{BB}$  and the cross-adhesion strength  $f_1^{AB} := f_c$ . See SI for further details and parameters.

To our great surprise, very small *cross-adhesion* strengths  $f_c$  between cells of different tissues (i.e.  $f_c \ll \min(f_1^{AA}, f_1^{BB})$ ) result in fundamentally different out-

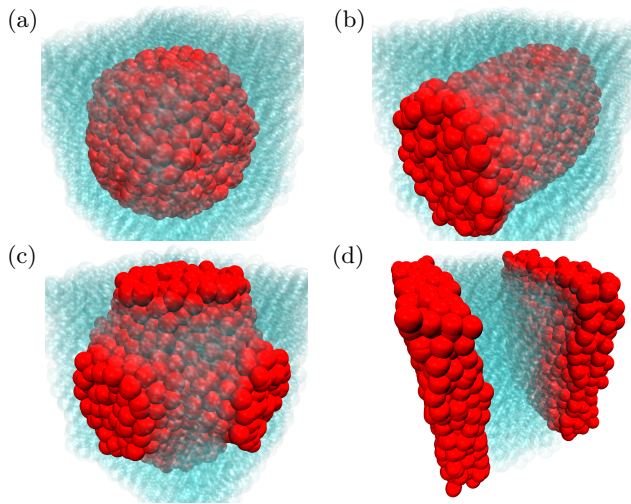


Fig. 1. Snapshots of various structures of tissue coexistence. (a) Spherical inclusion. (b) Cylindrical inclusion. (c) Schwarz-P like bicontinuous structure. (d) Flat interface. Other structures observed include perforated lamella, combinations (e.g. perforated lamellar together with a spheroid), and inverted (e.g. inverse spheroid) structures.

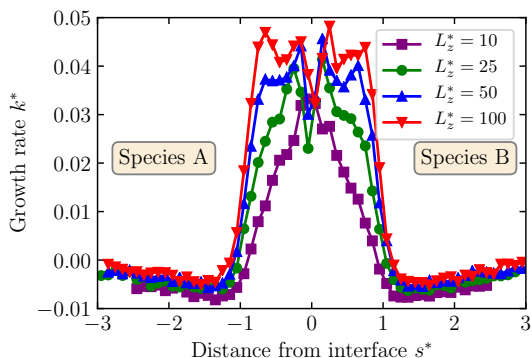


Fig. 2. Growth rate  $k^*$  as a function of the distance from the interface for the competition between two identical tissues with  $f_c = 0$  for different box lengths  $L_z^*$ .

comes of the tissue competition than predicted previously [31]. Instead of one tissue overwhelming the other or the existence of a critical size threshold explained above, we observe stable coexistence in a variety of different structures depending on initial conditions (see Fig. 1). Even for two identical tissues - just without cross-adhesion - a single A cell in a host of B grows into a stable spheroid occupying about a third of the volume. Similarly, a random 1:2 mixture of stronger A cells in a host of B can result in a stable 3:1 Schwarz-P bicontinuous structure.

In order to understand this puzzling behaviour and the underlying physical mechanisms, we turn to a simpler initial condition of a slab-like tissue arrangement and develop an appropriate analytic model. Cells are confined to a finite (periodic) compartment of size  $L_x \times L_y \times L_z$ . All cells in the central half ( $L_z/4 < z < 3L_z/4$ ) are type

B cells, all others type A. Large adhesion between cells of the same tissue and no adhesion between cells of different tissues leads to a large surface tension, stabilizing the flat interface. The division profile (see Fig. 2) reveals that cells divide more in a small region of width  $a$  (about one or two cell layers) at the interface. In the bulk of the tissue, the net growth is negative due to an elevated pressure. These results motivate a two-rate growth model [22–24, 32, 33]

$$\partial_t \rho + \nabla \cdot (\rho \mathbf{v}) = k_b \rho + \Delta k_s \Theta(s - a) \rho, \quad (2)$$

where  $\rho$  is the cellular density,  $\Theta$  the Heavyside step function,  $s$  the distance to the nearest interface and  $\mathbf{v}$  the cell-velocity field. The additional growth at the interface is modeled as a growth enhancement  $\Delta k_s$  near the interface (less than  $a$  away).

Division and apoptosis events locally relax stress and thus lead to a liquidification of the tissue on longer timescales [38–40]. Indeed, experiments on tissue rheology suggest liquid behaviour on long timescales [41–43], while some experiments on drosophila wing discs suggest that not all stress is relaxed by growth [44–46]. Our model tissue clearly behaves as a liquid [38]. With the low velocities and no external forcing, we can thus assume a constant pressure across the system. This motivates expanding  $k_b$  as in Eq. (1), and similarly  $\Delta k_s \simeq \Delta k_s^0 + \Delta k_s^1 (P_H - P)$ . Under the assumption of constant density and with an integration over the system, the time evolution of the cell number fraction  $\phi = N_A / (N_A + N_B)$  of type A cells reads

$$\partial_t \phi = k_b \phi + \Delta k_s \phi_s, \quad (3)$$

with the fraction  $\phi_s$  of A type cells at the surface. Two identical tissues (without cross-adhesion) then develop two interfaces  $L_z/2$  apart. Insertion of the linear expansions in Eq. (3) then yields the pressure

$$P = P_H + \frac{4a\Delta k_s^0}{(4a\Delta k_s^1 + \kappa L_z)}, \quad (4)$$

i.e. the additional growth at the interface elevates the pressure above the homeostatic pressure, which in turn causes the negative net growth rate in the bulk. We determine the bulk parameters  $P_H$ ,  $\kappa$  from bulk simulations as in Ref. [33], and the surface parameters  $a\Delta k_s^0$ ,  $a\Delta k_s^1$  by fitting Eq. (4) to a tissue with mirror boundary conditions in one direction (see SI). As shown in Ref. [33], the homeostatic pressure grows approximately linearly with  $G$ , and decreases linearly with  $f_1$ .  $\kappa$  is essentially independent off  $f_1$ , but decreases linearly with  $G$ . The surface parameter  $\Delta k_s^0$  is only weakly dependent on  $G$ , but grows linearly with  $f_1$ , while  $\Delta k_s^1$  does not show a clear dependence on tissue parameter (see SI). Representatively, we show the pressure dependence on box length  $L_z$  for two identical tissues without cross adhesion. With the

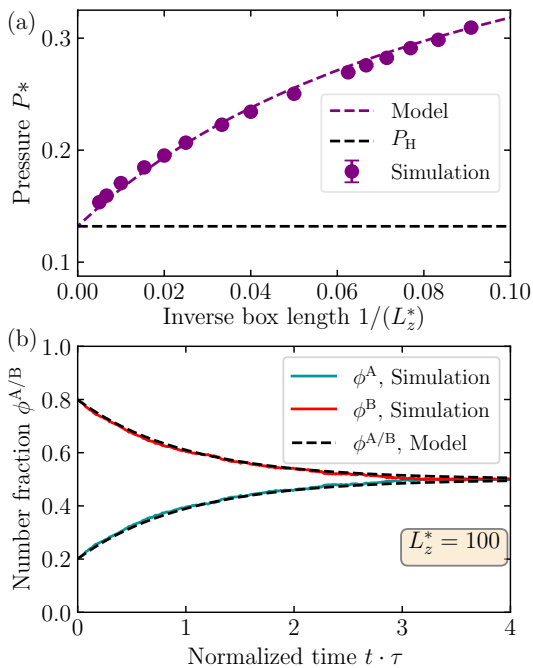


Fig. 3. (a) Average pressure measured in competitions between two identical tissue (reference tissue, see SI) with zero cross-adhesion  $f_c = 0$  in terms of the inverse box length  $L_z^*$ . Dashed purple line shows the prediction of the two-rate model according to Eq. (4). (b) Solid cyan and red lines show the time evolution of the cell number fractions  $\phi^{A/B}$  for a competition as in (a), for a box length  $L_z^* = 100$ . Dashed black line shows the prediction given by Eq. (5) for both tissues.

parameters fixed, the theory reproduces the simulations without further parameter adjustment (see Fig. 3(a)).

For identical tissues, the steady-state solution to Eq. (3) is  $\phi = 1/2$  by symmetry. For the dynamics we obtain

$$\phi(t) = \frac{1}{2} + (\phi_0 - \frac{1}{2})e^{-\kappa(P - P_H)t}, \quad (5)$$

with the initial number fraction  $\phi_0$ . As shown in Fig. 3(b), Eq. (5) reproduces the simulation dynamics.

Next, we explore the competition between two different tissues with a planar interface. We balance the pressures on both sides of the interface and get

$$P = P_H^A + \frac{2a\Delta k_s^{0A}}{(2a\Delta k_s^{1A} + \kappa^A L_A)} = P_H^B + \frac{2a\Delta k_s^{0B}}{(2a\Delta k_s^{1B} + \kappa^B L_B)}, \quad (6)$$

where  $L_B$  and  $L_A (= L_z - L_B)$  are the lengths occupied by tissue A and B. Note that inserting  $L_{A,B} < L_z$  in Eq. (6) gives a lower bound for the pressure: The system pressure is always larger than the homeostatic pressure of the stronger tissue, plus a system-size-dependent constant. Indeed, this lower bound describes the pressure rather well. The stronger tissue occupies the larger part of the system, and thus  $L_{A,B} \approx L_z$ . Thus the pressure is almost constant for  $\Delta P_H < 0$ , and grows almost linearly

for  $\Delta P_H > 0$  (see Fig. 4). The weaker tissue supports the higher pressure by decreasing in size, and thus its apoptotic volume, sustained by surface growth. For the simulated tissues, the parameter  $\kappa$ ,  $\Delta k_s^0$  and  $\Delta k_s^1$  only show small variations (see SI). We therefore assume them to be the same for both tissues in order to obtain

$$\phi = \frac{1}{2} + \frac{2a\Delta k_s^0}{\kappa(P_H^B - P_H^A)L_z} \pm \left[ \left( \frac{2a\Delta k_s^0}{\kappa(P_H^B - P_H^A)L_z} \right)^2 + \left( \frac{1}{2} + \frac{2a\Delta k_s^1}{\kappa L_z} \right)^2 \right]^{\frac{1}{2}}. \quad (7)$$

Note that for  $\Delta P_H \equiv (P_H^B - P_H^A) \rightarrow 0$ , Eq. (7) reproduces  $\phi = 1/2$  as expected. Around  $\Delta P_H = 0$ ,  $\phi$  grows linearly with  $\Delta P_H$  and then slows down (see Fig. 4). For large differences in homeostatic pressure, the model predicts two interfaces less than  $2a$  apart, thus violating its assumptions, and consequently fails to predict the simulation results properly. Equations (6) and (7) are able to reproduce simulation results fairly well without parameter adjustments (see Fig. 4) in a broad parameter regime. Note that this also holds true for negative homeostatic bulk pressures, where indeed the system pressure is positive, thanks to the surface growth (see Eq. (6)).

These results show that indeed the enhanced growth at the interface lies at the heart of the coexistence of tissues observed in our simulations. However, a flat interface is not the only stable structure for two competing tissues. Depending on initial conditions and parameters, a large range of other structures can be found (see Fig. 1). These different structures result in different surface-to-volume ratios (and possibly other interfacial effects), changing the steady-state volume fractions and pressures. We present simulation results for these structures in Fig. 5.

Compared to flat interfaces, the number fraction  $\phi$  of tissues in spherical or cylindrical configuration is smaller, with spheroids being smaller than cylinders. Note that spheroids become unstable with growing homeostatic pressure difference. They then turn into cylinders, which again become unstable and turn into a slab-like structure, which probably becomes unstable as well. Vice versa, cylinders turn into spheroids if the difference in homeostatic pressure is very negative. The number fraction of the bicontinuous phase is roughly the same as for flat interfaces, but the bicontinuous phase is only stable in a small regime of homeostatic pressure differences. For larger differences in homeostatic pressure it turns into a perforated lamella phase of the weaker tissue inside the stronger tissue. In general, the number fraction  $\phi$  of all structures changes sigmoidally with homeostatic pressure difference (see Fig. 1).

While all of these structures are very stable over time, the question arises how stable they are when the interfacial effects become smaller. We study this effect numerically, by observing the structures for two identical tissues

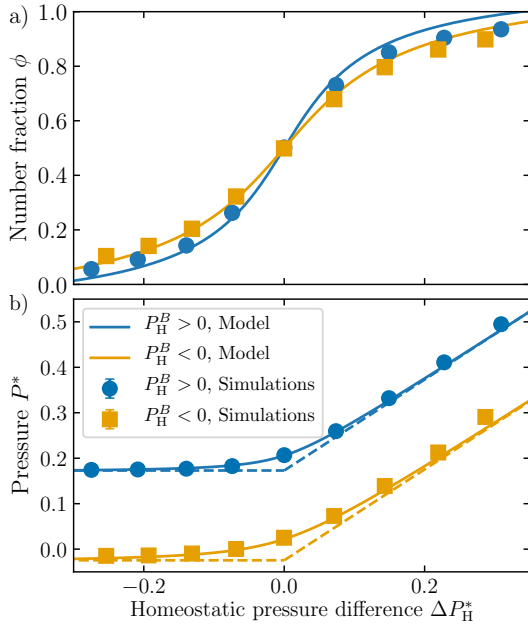


Fig. 4. (a) Cell number fractions  $\phi$  for various homeostatic pressure differences  $P_H^B - P_H^A$ . Tissue B is fixed (reference tissue) and the homeostatic pressure of tissue A is varied. Symbols are simulation results while the solid lines are predictions by the two-rate model according to Eq. (7), using the parameters of tissue B. Blue corresponds to positive homeostatic pressure of tissue B and yellow to a negative one. (b) Average pressure measured during the simulations shown in (a) together with a plot of Eq. (6), using the parameter of tissue B. Dashed lines are lower bounds from  $L_{A,B} < L_z$ . Boxsize  $L_x = L_y = 10; L_z = 40$

formed under zero cross-adhesion and continuously increase the cross-adhesion  $f_c$  to the value of self-adhesion (i.e.  $f_c = f_1^{AA} = f_1^{BB}$ ). Figure 6 shows that all structures remain almost unchanged up to a cross-adhesion  $f_c$  approximately two thirds of the self adhesion  $f_1$ . For higher  $f_c$  only a mixed, sponge-like state remains.

In summary, the interface between two tissues plays an important role in the competition between them. The enhanced growth at the interface can stabilize coexisting phases even when one tissue has a higher homeostatic pressure. The coexisting phase appears in a variety of different structures, ranging from a spherical inclusion over a flat interface to a bicontinuous phase.

Interesting future directions are interfacial dynamics, roughness, and shapes, as previously explored for tissues on substrates and without additional interfacial growth [34, 47, 48]. Vice versa, it would be interesting to add interfacial growth to tissues growing on substrates.

Finally, our results suggests a tentative explanation for tumor heterogeneity and the abundance of occult tumors: small symptom-free micro-tumors that are frequently found in the human body [49]. For the theyroid, it is indeed considered 'normal' to find microscopic lesions [50]. Our results provide a mechanical explanation

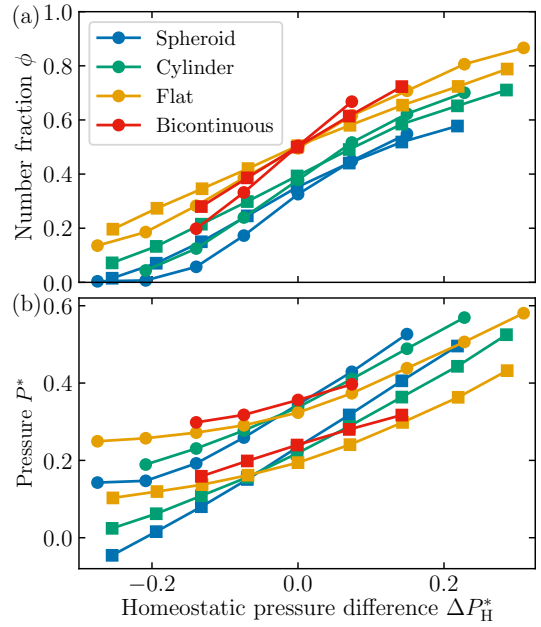


Fig. 5. Cell number fractions  $\phi$  for different homeostatic pressure differences  $\Delta P_H^*$  and different structures, as indicated by color. Circles correspond to a positive homeostatic pressure of tissues B and squares to a negative one (same parameters as in Fig. 4, except cubic box size  $L = 10$ ). (b) Average pressure measured in the simulations shown in (a)

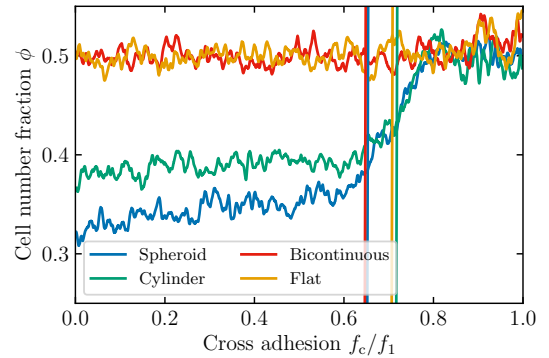


Fig. 6. Variation of cell number fraction  $\phi$  with time with increasing cross-adhesion  $f_c/f_1 = t^*/240$  between two identical tissues. Simulations are started from spherical (blue) and cylindrical inclusions (green) of tissue A in B as well as from flat interfaces (yellow) and a bicontinuous phase (red). Solid lines are marking transition points after which the corresponding initial structure forms a three dimensional percolated cluster. Cubic box size  $L = 10$

how coexistence of different tissues can be stable by simple mechanical effects. For example, a mutation might downregulate cadherins - an important cellular adhesion protein - as it often happens in tumors [51]. On the one hand, this might reduce survival signaling [52], but the lack of adhesion also favors our mechanism of coexistence, even for weaker tissue growth.

## ACKNOWLEDGEMENTS

The authors gratefully acknowledge the computing time granted through JARA-HPC on the supercomputer JURECA [53] at Forschungszentrum Jlich

- 
- [1] B. I. Shraiman, Proc. Natl. Acad. Sci. U. S. A. **102**, 3318 (2005).
- [2] M. A. Wozniak and C. S. Chen, Nat. Rev. Mol. Cell Biol. **10**, 34 (2009).
- [3] K. D. Irvine and B. I. Shraiman, Development **144**, 4238 (2017).
- [4] M. Jarvis, S. Briggs, and J. Knox, Plant Cell Environ. **26**, 977 (2003).
- [5] E. Coen, R. Kennaway, and C. Whitewoods, Development **144**, 4203 (2017).
- [6] S. Kumar and V. M. Weaver, Cancer Metastasis Rev. **28**, 113 (2009).
- [7] D. T. Butcher, T. Alliston, and V. M. Weaver, Nat. Rev. Cancer **9**, 108 (2009).
- [8] A. Taloni, M. Ben Amar, S. Zapperi, and C. A. La Porta, Eur. Phys. J. Plus **130**, 224 (2015).
- [9] A. J. Engler, S. Sen, H. L. Sweeney, and D. E. Discher, Cell **126**, 677 (2006).
- [10] C. M. Nelson, R. P. Jean, J. L. Tan, W. F. Liu, N. J. Sniadecki, A. A. Spector, and C. S. Chen, Proc. Natl. Acad. Sci. U.S.A. **102**, 11594 (2005).
- [11] G. Cheng, J. Tse, R. K. Jain, and L. L. Munn, PLoS One **4**, e4632 (2009).
- [12] J. Fink, N. Carpi, T. Betz, A. Betard, M. Chebah, A. Azioune, M. Bornens, C. Sykes, L. Fetler, D. Cuvelier, and M. Piel, Nat. Cell Biol. **13**, 771 (2011).
- [13] M. Uyttewaal, A. Burian, K. Alim, B. Landrein, D. Borowska-Wykret, A. Dedieu, A. Peaucelle, M. Ludynia, J. Traas, A. Boudaoud, D. Kwiatkowska, and O. Hamant, Cell **149**, 439 (2012).
- [14] S. J. Streichan, C. R. Hoerner, T. Schneidt, D. Holzer, and L. Hufnagel, Proc. Natl. Acad. Sci. U.S.A. **111**, 5586 (2014).
- [15] L. LeGoff and T. Lecuit, Cold Spring Harbor Perspect. Biol. **8**, a019232 (2015).
- [16] D. Eder, C. Aegerter, and K. Basler, Mech. Dev. **144**, 53 (2017).
- [17] G. Helmlinger, P. A. Netti, H. C. Lichtenbeld, R. J. Melder, and R. K. Jain, Nat. Biotechnol. **15**, 778 (1997).
- [18] V. D. Gordon, M. T. Valentine, M. L. Gardel, D. Andor-Ardo, S. Dennison, A. A. Bogdanov, D. A. Weitz, and T. S. Deisboeck, Exp. Cell Res. **289**, 58 (2003).
- [19] L. J. Kaufman, C. P. Brangwynne, K. E. Kasza, E. Filippidi, V. D. Gordon, T. S. Deisboeck, and D. A. Weitz, Biophys. J. **89**, 635 (2005).
- [20] K. Alessandri, B. R. Sarangi, V. V. Gurchenkov, B. Sinha, T. R. Kiesling, L. Fetler, F. Rico, S. Scheuring, C. Lamaze, A. Simon, S. Geraldo, D. Vignjevic, H. Domejean, L. Rolland, A. Funfak, J. Bibette, N. Bremond, and P. Nassoy, Proc. Natl. Acad. Sci. U.S.A. **110**, 14843 (2013).
- [21] H. Domejean, M. d. l. M. Saint Pierre, A. Funfak, N. Atrux-Tallau, K. Alessandri, P. Nassoy, J. Bibette, and N. Bremond, Lab. Chip **17**, 110 (2017).
- [22] F. Montel, M. Delarue, J. Elgeti, L. Malaquin, M. Basan, T. Risler, B. Cabane, D. Vignjevic, J. Prost, G. Cappello, and J. F. Joanny, Phys. Rev. Lett. **107**, 188102 (2011).
- [23] F. Montel, M. Delarue, J. Elgeti, D. Vignjevic, G. Cappello, and J. Prost, New J. Phys. **14**, 055008 (2012).
- [24] M. Delarue, F. Montel, O. Caen, J. Elgeti, J.-M. Siaugue, D. Vignjevic, J. Prost, J.-F. Joanny, and G. Cappello, Phys. Rev. Lett. **110**, 138103 (2013).
- [25] A. Taloni, A. A. Alemi, E. Ciusani, J. P. Sethna, S. Zapperi, and C. A. M. La Porta, PLoS One **9**, e94229 (2014).
- [26] G. Morata and P. Ripoll, Dev. Biol. **42**, 211 (1975).
- [27] B. Diaz and E. Moreno, Exp. Cell Res. **306**, 317 (2005).
- [28] S. H. Moolgavkar and E. G. Luebeck, Genes. Chromosomes Cancer **38**, 302 (2003).
- [29] R. Meza and J. T. Chang, BMC Public Health **15**, 789 (2015).
- [30] L. Hufnagel, A. A. Teleman, H. Rouault, S. M. Cohen, and B. I. Shraiman, Proc. Natl. Acad. Sci. U. S. A. **104**, 3835 (2007).
- [31] M. Basan, T. Risler, J.-F. Joanny, X. Sastre-Garau, and J. Prost, HFSP J **3**, 265 (2009).
- [32] M. Basan, J. Prost, J.-F. Joanny, and J. Elgeti, Phys. Biol. **8**, 026014 (2011).
- [33] N. Podewitz, M. Delarue, and J. Elgeti, Europhys. Lett. **109**, 58005 (2015).
- [34] N. Podewitz, F. Jülicher, G. Gompper, and J. Elgeti, New J. Phys. **18**, 083020 (2016).
- [35] N. Jagiella, B. Mueller, M. Mueller, I. E. Vignon-Clementel, and D. Drasdo, PLoS Comput. Biol. **12**, 1 (2016).
- [36] P. Van Liedekerke, M. M. Palm, N. Jagiella, and D. Drasdo, Comput. Part. Mech. **2**, 401 (2015).
- [37] Y. Kobayashi, Y. Yasugahira, H. Kitahata, M. Watanabe, K. Natsuga, and M. Nagayama, npj Comput. Mater. **4**, 45 (2018).
- [38] J. Ranft, M. Basan, J. Elgeti, J.-F. Joanny, J. Prost, and F. Jülicher, Proc. Natl. Acad. Sci. U. S. A. **107**, 20863 (2010).
- [39] N. Khalilgharibi, J. Fouchard, P. Recho, G. Charras, and A. Kabla, Curr. Opin. Cell Biol. **42**, 113 (2016).
- [40] D. A. Matoz-Fernandez, E. Agoritsas, J.-L. Barrat, E. Bertin, and K. Martens, Phys. Rev. Lett. **118** (2017).
- [41] H. Phillips and M. Steinberg, J. Cell Sci. **30**, 1 (1978).
- [42] K. Guevorkian, M.-J. Colbert, M. Durth, S. Dufour, and F. Brochard-Wyart, Phys. Rev. Lett. **104**, 218101 (2010).
- [43] D. Gonzalez-Rodriguez, L. Bonnemay, J. Elgeti, S. Dufour, D. Cuvelier, and F. Brochard-Wyart, Soft Matter **9**, 2282 (2013).
- [44] L. LeGoff, H. Rouault, and T. Lecuit, Development **140**, 4051 (2013).
- [45] Y. Mao, A. L. Tournier, A. Hoppe, L. Kester, B. J. Thompson, and N. Tapon, The EMBO journal **32**, 2790 (2013).
- [46] Y. Pan, I. Heemskerk, C. Ibar, B. I. Shraiman, and K. D. Irvine, Proc. Natl. Acad. Sci. U.S.A. **113**, E6974 (2016).
- [47] J. Ranft, M. Aliee, J. Prost, F. Jülicher, and J.-F. Joanny, New J. Phys. **16**, 035002 (2014).
- [48] J. J. Williamson and G. Salbreux, (2017).
- [49] M. J. Bissell and W. C. Hines, Nat. Med. **17**, 320 (2011).
- [50] H. R. Harach, K. O. Franssila, and V. M. Wasenius, Cancer **56**, 531 (1985).
- [51] R. A. Weinberg, *The biology of cancer* (Garland Publishing, Inc., 2007).

- [52] Alberts, Bray, Johnson, Lewis, Raff, Roberts, and Watson, *Molecular Biology of the Cell, 3rd edition* (Garland Publishing, Inc., 1994).
- [53] Jülich Supercomputing Centre, Journal of large-scale research facilities **4** (2018).